

Effect of Buffer Layer on Crack Susceptibility, Mechanical and Microstructural Properties of Ni Hard Coatings



Nikhil Thawari, Nikhil Chaubey, Aayush Chandak, and T. V. K. Gupta

1 Introduction

Laser cladding process is a hard coating technique being widely used due to its potential in material processing such as high-value component repair, metallic coating, small volume production and prototyping [1]. The process uses laser as a heat source which creates a melt pool over the substrate producing a hard-coated/deposited layer [2] as shown in Fig. 1. There are two ways of powder feeding in this process, i.e. pre-placed and co-axial, where co-axial feeding is commonly used that can provide uniform flow to the laser source creating a uniform deposition. Some of the advantages of laser cladding are less dilution, minimum distortion and heat-affected zone (HAZ), low heat input to the substrate, higher accuracy, etc. [3, 4]. The process is primarily used for refurbishment and rebuilding of worn-out parts and make them sustainable to work in harsh environments and perform their function at a satisfactory level to enhance the component service life [5–7]. Nickel-based alloys are widely deposited with laser cladding to produce high heat resistant coatings. N480 and N9062 are specialized Ni-based alloys, where N480 possesses medium hardness (500HV), good abrasion and corrosion resistance with a reasonable impact resistance, and N9062 has higher hardness (750HV), excellent abrasion resistance, low ductility which provides low impact resistance. Both the coatings are better for wear and corrosion resistance applications. Whereas, the deposition of these hard coatings by laser cladding generates cracks, dilution and residual stresses because of which extensive research is in progress to minimize these problems [8–11].

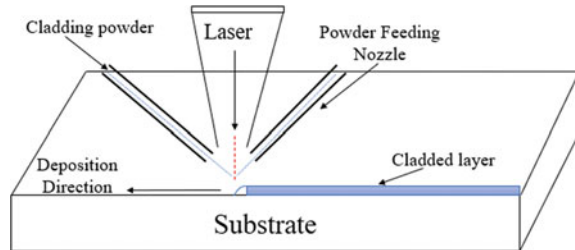
N. Thawari · N. Chaubey · T. V. K. Gupta (✉)

Mechanical Engineering, Visvesvaraya National Institute of Technology, Nagpur 440010, India
e-mail: tvkgupta@mec.vnit.ac.in

A. Chandak

Shreenath Engineering Industries, MIDC-Higna, Nagpur 440016, India
e-mail: aayush.chandak@shreenath-industries.com

Fig. 1 Laser cladding process



Stanciu et al. [12] deposited a dual coating of NiCrBSi with Inconel718 as buffer layer using laser cladding and reported that crack susceptibility of the top layer is reduced since the compressive stresses are reduced with uniform heat distribution. Also, a significant increase in hardness with 7% increase in wear resistance and 20% in corrosion resistance are claimed. Another study on crack behaviour of composite coating of Ni-based WC by Zhou et al. [13] revealed dissolution of cladded particles is minimized at high scanning speeds and the increased preheating reduced the temperature gradients to obtain crack-free cladding. Wang et al. [14] investigated the crack susceptibility and microstructural behaviour of V_2O_5 /NiCrBSi alloys and observed that the thermal stresses govern the crack occurrence. Also, Doliveira et al. [15] found that buffer layer addition in multilayer cladding reduces the tensile residual stresses which may lead to early failure of the component. Thawari et al. [16] added Inconel 625 as buffer layer while cladding Stellite 6 and observed higher hardness and wear resistance as compared to direct Stellite 6 deposition. Also, cladding on Fe-based substrate, dilution of Fe elements increases the rise of crack formation and also deteriorates the mechanical and microstructural properties of the coating [17, 18].

The literature proposed different methods to minimize the crack susceptibility of hard coatings where the substrate was pre-heated to reduce the crack formation [19–21], while this method can only be recommended if the coefficient of thermal expansion of the cladding material and substrate is not vastly different. Reports also revealed that addition of buffer layer reduces the crack formation, also enhances the mechanical and microstructural properties of different hard coatings, showing improved results than the direct deposition. Despite this research reported, no study was available on buffer layer addition in cladding of Ni-based hard alloys. To fill this gap and investigate the role of buffer layer addition, an attempt was made by cladding Inconel 625 between the substrate and Ni-based alloys to reduce the crack susceptibility, dilution and enhance the properties of N480 and N960 coatings. It was found that buffer layer plays a vital role in reducing the possibility of crack formation and reduced substrate element diffusion into the hard-deposited layers.

Table 1 Chemical composition (% by weight)

Material	Ni	Cr	B	Si	C	Fe	Mo	Cu	W	Co	Nb	Others
Inconel 625	58.0	20–23	–	–	–	5.0	8–10	–	–	1	3.15	2–5
N480	39.8	13.0	2.5	3.4	0.45	4.5	5.9	1.36	29.0	–	–	–
N9062	72.4	15.5	2.9	4.3	0.7	4.2	–	–	–	–	–	–
SS410	–	11.5–13.5	–	1.0	0.15	84–86	–	–	–	–	–	–

2 Experimental Set-Up

2.1 Cladding and Substrate Material

In the present work, N480 and N9062 (Ni alloys) were used as hard coatings with Inconel 625 as buffer layer (particle size 30–100 μm) for experimentation. The substrate is a hollow cylindrical sleeve made of AISI SS410 martensitic stainless steel with 115 mm length, 34 mm and 50 mm inner and outer dia., respectively. Table 1 gives the chemical composition of Inconel 625, N480, N9062 and SS410.

2.2 Experimental Procedure

All the experiments are performed with a fibre-coupled diode laser (Model Laserline LDF 4000–100) having max. output power of 4 kW. The laser beam is focused perpendicular to the substrate surface at a distance of 20 mm with clad materials being fed (M/s Suzlor Metco) through a co-axial nozzle into the processing region. The devices, i.e. optics and nozzles, are integrated with a 6 DOF KUKA KR16 robotic arm controlled by a central computer. Argon is used as a carrier and shielding gas to deliver the powders and also to protect the cladding zone from oxidation. During the experimentation, the optimum process parameters are used, i.e. laser power—2.8 KW, powder feed rate—46 g/min and scanning speed—20 mm/sec for cladding buffer, N480 and N9062 layers.

Initially, Inconel 625 powder as the buffer layer was cladded on two different samples and further allowed to cool to room temperature. Then, N480 and N9062 powders were deposited over the Inconel 625 creating a hard layer. The samples were pre-heated to 180–200 °C before cladding, and the cladded samples are shown in Fig. 2.



Fig. 2 Laser cladded samples

Table 2 Micro-hardness of N9062 and N480 along the depth direction

Distance from top surface (mm)	0	0.25	0.5	0.75	1.0	1.25	1.5
N9062 Micro-hardness (HV)	797	808	843	848	831	814	716
N480 Micro-hardness (HV)	608	616	635	598	522	–	–

2.3 Characterization and Micro-hardness Measurement

The samples are transversely cut with electric discharge machine (EDM) for microstructural characterization. The specimens are mirror polished using various grades (from 120 to 2500) of abrasive/sandpapers followed by velvet cloth polishing. Before performing the microstructural characterization through SEM, the samples are etched with a mixture of HF and HNO₃ in the ratio of 3:7 for about 5–8 s. The micro-hardness along the clad thickness (radial direction) is measured using TUKON 2100 Wolpert, INSTRON Vickers micro-hardness tester at a load of 300 g for 15 s, and the results obtained are given in Table 2.

3 Results and Discussion

3.1 Micro-hardness

In this study, before measuring the micro-hardness of cladded buffer layer, N480 and N9062, SEM micrograph at different locations using multiple point dimension were taken, whereas no tracks are observed from the optical images as shown in Fig. 5a, d. From the results, an average clad height of 1.3, 1.01 and 1.50 mm are obtained for buffer layer, N480 and N9062, respectively. The graph plotted in Fig. 3 shows the specimen micro-hardness variation along the depth direction. Each reading represents an average of three readings. The maximum hardness was found to be just below the coating surface and reduced near the interface (hard coating and buffer layer). This

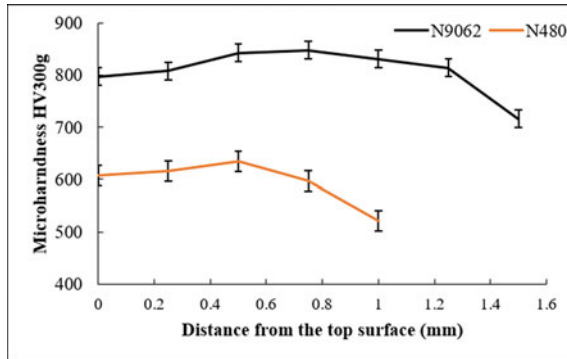


Fig. 3 Micro-hardness variation along the radial direction in N9062 and N480 coating

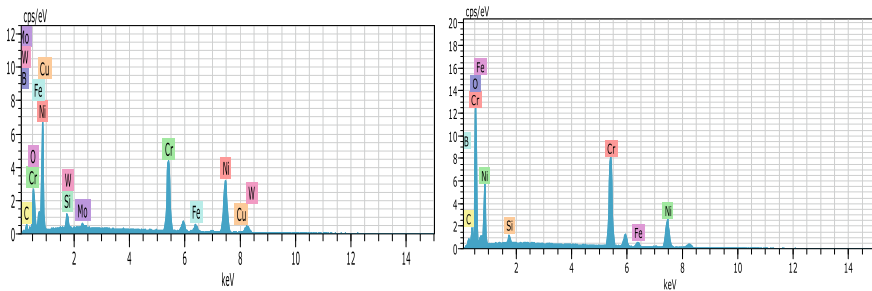


Fig. 4 EDS of N480 and N9062 hard coating layers at the middle of cladding

is due to the diffusion of some elements from the buffer layer. It is predicted that the high heat resistance property of Inconel 625 (buffer layer) resulted in smaller penetration depth of hard coatings over Inconel 625. Hence, the diffusion of Inconel 625 elements into the hard coatings was reduced as compared to the substrate material which decreases the dilution and maintains a good chemical composition as observed in EDS (Fig. 4). A 5–7% increase in hardness is obtained after cladding as compared to the original one. The higher hardness in the coating is due to the formation of hard carbides during cladding, which is also observed in SEM characterization.

3.2 Crack Formation

Most of the cracks in laser cladded components are because of the difference in thermal expansion coefficients of the substrate and coated materials. A buffer layer having an intermediate expansion coefficient reduces the thermal gradient during the cooling process in cladding. The heat transfers from the top layer to buffer layer at a different rate than the heat transfer between the buffer and substrate, due to different

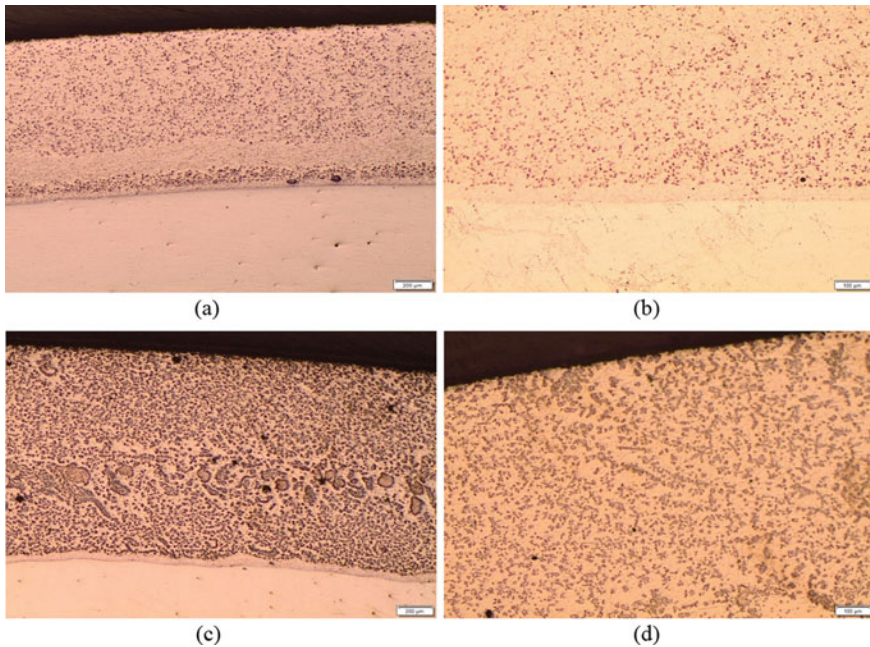


Fig. 5 Optical images. **a** N480 coating with buffer layer and substrate. **b** No crack initiation in hard coating. **c** N9062 coating with buffer layer and substrate. **d** No crack initiation in hard coating

thermal conductivities and heat resistivity of coated and the substrate materials. As a result, the buffer layer acts as a heat sink ensuring more uniform cooling as compared to direct deposition [12]. This induces compressive thermal stresses within the layer which decreases the chances of crack formation in the clad. Figure 5 also confirms hard-coated layer with no cracks in the optical measurements. Also, the crack formation is eliminated because the substrate is pre-heated to 180–200 °C prior cladding to reduce the solidification rate. At higher solidification rates, some amount of powder will not able to melt and mix properly with other elements in the melt pool which also results in cracks and other defects. The dispersion of hard (refractory) phases in N480 and N9062 coatings is more homogenous when a buffer layer is present than in direct cladding.

3.3 *Microstructural Characterization*

The SEM micrographs of the clad region with buffer layer for both the coatings are placed in Fig. 6. The image shows that the cladding is mainly composed of fine equi-axial dendritic structures. The presence of Cr_{23}C_6 and Cr_2C_7 carbides in Ni-rich dendrite matrix is responsible for higher hardness. These are found at the outer side

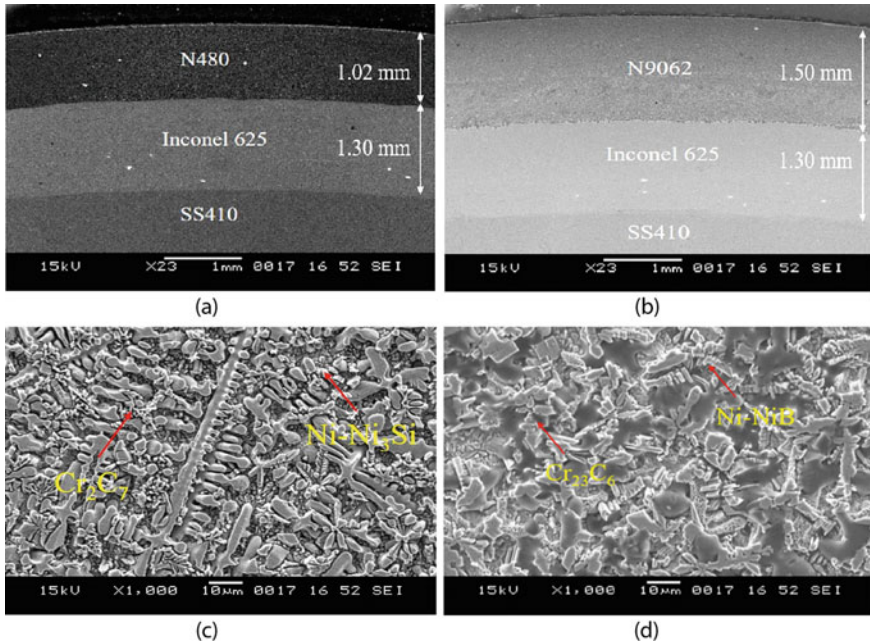


Fig. 6 **a** N480 coating with buffer layer and substrate. **b** N9062 coating with buffer layer and substrate. **c** Microstructural image of N480 hard coating. **d** Microstructural image of N9062 hard coating

of the grain boundaries. Inter dendritic eutectics of Ni-NiB is formed in N9062 layer while Ni-Ni₃Si in N480 as the quantity of Ni is higher in N9062 as compared to N480. The microstructure shows that near to the diffusion zone, columnar and free precipitation dendrites are present. The coarse needle-like structure of CrB precipitates near the overlapping zone is seen, due to the dilution by buffer layer elements. These precipitates have a pessimistic effect on hardness and crack susceptibility of the metal matrix. The buffer layer acts as a heat sink between the hard coating and substrate, thus reducing the thermal gradient which gave a fine grain structure.

The EDS analysis along the thickness was performed to know the effect of dilution on major alloying elements mainly Cr, Si, B, Mo on N480 and N9062. The EDS data shows that the weight % of the alloying element is reduced from top to near interface region as amount of buffer layer element; i.e. Ni is increased in the clad due to dilution. As a result, less carbides are formed and hence sudden fall in micro-hardness is observed near the interface which is still lower as compared to direct deposition.

4 Conclusions

Laser cladding of N480 and N9062 alloys with Inconel 625 as buffer layer on SS410 substrate was performed successfully. The following conclusions can be made based on the experiments and microstructural analysis:

- The buffer layer addition increases the micro-hardness of the hard coating depositions.
- Buffer layer also reduces the diffusion and dilution of the substrate elements into hard coating which increases wear and corrosion resistance of substrate.
- Uniform thermal gradients are observed in the hard coating with buffer layer, thus reducing the chances of crack formation.

Acknowledgements The authors acknowledge DST, Government of India for the financial support and testing equipment under Project No. DST/ECR/2016/001403.

References

1. Toyserkani, E., Khajepour, A., Corbin, S.F.: Laser Cladding. CRC (2004)
2. Kumar, V., Rakshit, R., Das, A.K.: Mechanical and tribological performance of fiber laser clad h-BN+ SS316 composite on SS316 surface. *J. Mater. Process. Technol.* **278**, 116509 (2020)
3. Jendrzejewski, R., Navas, C., Conde, A., de Damborenea, J.J., Sliwinski, G.: Properties of laser-clad stellite coatings prepared on preheated chromium steel. *Mater. Des.* **29**(1), 187–192 (2008)
4. Feng, K., Chen, Y., Deng, P., Li, Y., Zhao, H., Lu, F., Li, Z.: Improved high-temperature hardness and wear resistance of Inconel 625 coatings fabricated by laser cladding. *J. Mater. Process. Technol.* **243**, 82–91 (2017)
5. Song, L., Zeng, G., Xiao, H., Xiao, X., Li, S.: Repair of 304 stainless steel by laser cladding with 316L stainless steel powders followed by laser surface alloying with WC powders. *J. Manuf. Process.* **24**, 116–124 (2016)
6. Liu, H., Hu, Z., Qin, X., Wang, Y., Zhang, J., Huang, S.: Repair of 304 stainless steel by laser cladding with 316L stainless steel powders followed by laser surface alloying with WC powders. *Int. J. Adv. Manuf. Tech.* **91**(9–12), 3967–3975 (2017)
7. So, H., Chen, C.T., Chen, Y.A.: Wear behaviours of laser-clad stellite alloy 6. *Wear* **192**(1–2), 78–84 (1996)
8. Aubry, P., Blanc, C., Demirci, I., Dal, M., Malot, T., Maskrot, H.: Laser cladding and wear testing of nickel base hard facing materials: Influence of process parameters. *J. Laser Appl.* **29**(2), 022504 (2017)
9. Näkki, J., Tuominen, J., Vuoristo, P.: Effect of minor elements on solidification cracking and dilution of alloy 625 powders in laser cladding. *J. Laser Appl.* **29**(1), 012014 (2017)
10. Vostrak, M., Houdková, Š., Hruška, M.: Comparison of WC and (TiW) C in nickel-based alloy coatings prepared by laser cladding. *Int. IOP Conf. Ser. Mater. Sci. Eng.* **461**, 012092 (2019)
11. Korsmik, R.S., Turichin, G.A., Klimova-Korsmik, O.G., Alekseeva, E.V., Novikov, R.S.: Development of laser powder cladding technology for restoration of heat-resistant nickel alloys turbine blades. *J. Phys. Conf. Ser.* **1109**, 12–23 (2018)

12. Stanciu, E.M., Pascu, A., Țierean, M.H., Voiculescu, I., Roată, I.C., Croitoru, C., Hulka, I.: Dual coating laser cladding of NiCrBSi and Inconel 718. *Mater. Manuf. Process.* **31**(12), 1556–1564 (2016)
13. Zhou, S., Zeng, X., Hu, Q., Huang, Y.: Analysis of crack behavior for Ni-based WC composite coatings by laser cladding and crack-free realization. *Appl. Surf. Sci.* **255**(5), 1646–1653 (2008)
14. Wang, D.S., Liang, E.J., Chao, M.J., Yuan, B.: Investigation on the microstructure and cracking susceptibility of laser-clad V₂O₅/NiCrBSiC alloy coatings. *Surf. Coat. Technol.* **202**(8), 1371–1378 (2008)
15. Huang, Y., Zeng, X.: Investigation on cracking behavior of Ni-based coating by laser-induction hybrid cladding. *Appl. Surf. Sci.* **256**(20), 5985–5992 (2010)
16. Thawari, N., Gullipalli, C., Katiyar, J.K., Gupta, T.V.K.: Influence of buffer layer on surface and tribomechanical properties of laser clad stellite 6. *Mat. Sci. Eng. B.* **263**, 114799 (2021)
17. Sun, S., Durandet, Y., Brandt, M.: Parametric investigation of pulsed Nd: YAG laser cladding of stellite 6 on stainless steel. *Surf. Coat. Technol.* **194**(2–3), 225–231 (2005)
18. Lin, W.C., Chen, C.: Characteristics of thin surface layers of cobalt-based alloys deposited by laser cladding. *Surf. Coat. Technol.* **200**(14–15), 4557–4563 (2006)
19. Luo, X., Li, J., Li, G.J.: Effect of NiCrBSi content on microstructural evolution, cracking susceptibility and wear behaviors of laser cladding WC/Ni–NiCrBSi composite coatings. *J. Alloys Compd.* **626**, 102–111 (2015)
20. D'Oliveira, A.S.C., da Silva, P.S.C., Vilar, R.M.: Microstructural features of consecutive layers of stellite 6 deposited by laser cladding. *Surf. Coat. Technol.* **153**(2–3), 203–209 (2002)
21. Fallah, V., Alimardani, M., Corbin, S.F., Khajepour, A.: Impact of localized surface preheating on the microstructure and crack formation in laser direct deposition of stellite 1 on AISI 4340 steel. *Appl. Surf. Sci.* **257**(5), 1716–1723 (2010)